Available online at www.sciencedirect.com
SCIENCE DIRECT
Catalysis Today 116 (2006) 216–225
CATALYSIS TODAY
www.elsevier.com/locate/cattod

Understanding the role of nitridation in butan-1-ol and butan-2-ol dehydration mechanisms over oxynitrides

S. Delsarte [a,*], M. Florea [b], F. Maugé [c], P. Grange [a,✠]

[a] *Catalyse et chimie des matériaux divisés, Université Catholique de Louvain, 2/17 Croix du Sud, 1348 Louvain-la-Neuve, Belgium*
[b] *University of Bucharest, Dept. Chem. Techn & Catalysis, B-dul R. Elisabeta 4-12, Bucharest 70346, Romania*
[c] *Catalyse et Spectrochimie, CNRS UMR 6506, ENSICEAN, 6 bd du Maréchal Juin, 14050 Caen cedex, France*

Available online 6 June 2006

Abstract

Conversions and selectivities of butan-2-ol and butan-1-ol dehydration were studied over a series of five AlGaPO(N) samples with increasing nitrogen contents (0, 5.3, 11.0, 15.9 and 23.3 wt.%) in a conventional continuous flow micro-reactor system at 200 and 275 °C for butan-2-ol and butan-1-ol dehydration, respectively. Those reactions were chosen as test reactions of the changes induced by nitridation on the acid, base and bifunctional acid–base properties of AlGaPON under catalytic conditions. The catalytic properties of the AlGaPO phosphate precursor are compared to those of the four nitrided phosphates and the influence of nitridation on the initial activities, selectivities and on the stability of the catalysts are discussed in relation to the changes induced by nitridation on their acid–base properties.

Cis- and *trans*-2-butene are the main reaction products from butan-2-ol dehydration, indicating an E2 elimination mechanism, with a strong E1 character. The number of active sites for butan-2-ol dehydration decreases with nitrogen enrichment, in parallel with the number of acid sites evaluated by ammonia chemisorption experiments.

Dibutylether is the main reaction product from butan-1-ol dehydration, indicating that two alcohol molecules can be activated simultaneously on adjacent acid and base sites. The number of acid–base conjugated sites catalysing the intermolecular dehydration of butan-1-ol is increased at the beginning of nitridation, but an optimum density of sites is attained for intermediate nitrogen contents.

To determine the nature of the surface species interacting with the reactants, we compare the FT-IR spectra recorded before and after methanol and butan-1-ol adsorption.

Keywords: Butanol dehydration; Bifunctional acid–base catalysis; AlGaPON; Oxynitrides

1. Introduction

When nitrogen atoms are introduced to substitute oxygen in a phosphate network, the acidity of the initial solid is decreased, while base sites are created on the surface. This has been evidenced in our laboratory for the substitution of oxygen by nitrogen in $AlPO_4$ [1–3], $Al_{0.5}Ga_{0.5}PO_4$ [4,5] and $Zr_{0.9}PO_{4.3}$ [6,7], by means of acid (SO_2, $CDCl_3$) and base (NH_3, C_5H_5N) probes.

A direct correlation between the number of base sites, evaluated by SO_2 microcalorimetry, and the total nitrogen content of the samples was observed for AlPON, AlGaPON and ZrPON. Another strategy to characterize the basicity of catalysts, is to use a test reaction known to be catalysed by liquid bases, as for instance the Knoevenagel condensation between benzaldehyde and malononitrile. We measured the activity of AlPON, AlGaPON and ZrPON series of samples under the same conditions. For the ZrPON series of samples, a progressive increase of the activity with nitrogen enrichment was observed. For AlPON and AlGaPON, the correlation was not so obvious, and the least nitrided samples of the series were the most active. Up to know, this apparent discrepancy between SO_2 microcalorimetry experiments and the reaction rates measured for the Knoevenagel condensation could not be explained. In Refs. [4,5], we suggested that the high activity of the weakly nitrided oxynitrides was due to a high superficial concentration of chemisorbed ammonia. Since then, we have put in evidence, on AlPON, the existence of coupled acid–base sites, able to interact simultaneously with the acid and base

* Corresponding author. Tel.: +32 10 47 36 50; fax: +32 10 47 36 49.
E-mail address: gueguenerw@yahoo.fr (S. Delsarte).
✠ Deceased 11 July 2003.

0920-5861/$ – see front matter © 2006 Elsevier B.V. All rights reserved.
doi:10.1016/j.cattod.2006.01.033

functional groups of the reactants by means of alcohol dehydration reactions [8]. The density of such sites increases at the beginning of nitridation, but decreases for nitrogen contents higher than 11%. The presence, on weakly nitrided AlPON, of acid sites capable of activating the carbonyl group of benzaldehyde, while the proton of malononitrile is abstracted by an adjacent base site, could explain the particularly high activity of this sample for the Knoevenagel condensation reaction.

On AlGaPON, the presence of coupled acid–base sites was postulated to explain their good performances as support for platinum for the dehydrogenation of isobutane to isobutene [9].

The aim of the present study is to confirm the existence of coupled acid and base sites on AlGaPON and to determine the evolution of the density of those sites with nitrogen enrichment, in order to verify that their density is maximum for the weakly nitrided samples. We will show that the findings on AlPON can be extrapolated to another family of nitrided phosphates. The tested series contains five samples: one oxide and four oxynitrides. The strategy will be to study the evolution of the activity and selectivity of those samples for the dehydration of butan-1-ol and butan-2-ol, as both reactions can proceed over coupled acid–base sites and to confront the catalytic results with those obtained in the past by ammonia chemisorption and sulphur dioxide microcalorimetry experiments. To determine the nature of the surface species interacting with the reactants, we compared the FT-IR spectra recorded before and after methanol and butan-1-ol adsorption. The stability of the catalysts is also discussed.

2. Methods

2.1. Materials

The high surface area, amorphous $Al_{0.5}Ga_{0.5}PO_4$ precursor was synthesised by a process developed by Kearby [10] for aluminophosphates and adapted for the "(Al, Ga)PO" compositions [11]. A solution of adequate amounts of Ga^{3+}, Al^{3+} and H_3PO_4 2 M (Ga + Al)/P and Ga/Al atomic ratios of 1 was cooled at 0 °C in a dry ice-alcohol bath. Then, a large excess of propylene oxide was slowly added under vigorous stirring. After some hours at room temperature, a translucent gel was produced. The gel was washed with isopropanol and dried at 110 °C. The resulting powder was sieved ($Ø < 100$ μm) and calcined in air at 650 °C. The precursor, placed in the isothermal region of a tubular furnace, was activated under ammonia flow (30 l h^{-1}) at 750 °C. This reaction allows the progressive substitution of oxygen by nitrogen according to Eq. (1):

$$Ga_{0.5}Al_{0.5}PO_4 + yNH_3 \rightarrow Ga_{0.5}Al_{0.5}PO_{(4-3y/2)}N_y + 3y/2H_2O \quad (1)$$

Various nitrogen contents were obtained by modifying the time of nitridation from 3 to 89 h. At the end of the activation process, the samples were cooled down to room temperature under pure and dry nitrogen flow.

The total nitrogen content of the AlGaPON samples was determined by titration with a sulphuric acid solution of the ammonia liberated in alkaline digestion at 400 °C with melted KOH [12]. The specific surface area was measured by the single-point BET method in a Micromeritics Flowsorb II 2300 apparatus, after 20 min degassification at 250 °C. The nitridation conditions and the main characteristics of the studied AlGaPON are presented in Table 1. All samples are X-ray amorphous white powders. The compositions of the nitrided samples presented in Table 1 were established from the total nitrogen content of the samples. Indeed, it has been shown that the Al/Ga and (Al + Ga)/P ratios were maintained during nitridation at 750 °C, and that the weight-loss recorded during nitridation corresponds to the replacement of three oxygen atoms by two nitrogen atoms [11].

The main physico-chemical properties of the reference oxide catalysts are presented in Table 2, as well as data relative to their synthesis procedure.

Table 1
Characteristics of the oxide and oxynitride AlGaPO(N) powders

Catalyst	Composition	Nitridation time (h)	Weight nitrogen content (wt.%)	S_{BET} (m^2/g)
AlGaPO	$Al_{0.5}Ga_{0.5}PO_4$	–	–	240
AlGaPON1	$Al_{0.5}Ga_{0.5}PO_{3.22}N_{0.52}$	3	5.3	150
AlGaPON2	$Al_{0.5}Ga_{0.5}PO_{2.43}N_{1.04}$	8	11.0	160
AlGaPON3	$Al_{0.5}Ga_{0.5}PO_{1.81}N_{1.46}$	16	15.9	145
AlGaPON4	$Al_{0.5}Ga_{0.5}PO_{0.94}N_{2.04}$	89	23.3	170

Table 2
Reference oxide catalysts characteristics

Catalyst	S_{BET} (m^2/g)	Structure	Synthesis procedure	Related literature
SiO_2–Al_2O_3 (6.38 wt.% Al)	370	Amorphous	Co-gel	
$AlPO_4$	118	Amorphous	Citrate complexation	[18]
Al_2O_3	339	Amorphous	Sol–gel	[19]
ZrO_2	88	Baddeleyite	Microwave-assisted synthesis	[20]
MgO	63	Periclase	Citrate complexation	[21]

2.2. X-ray photoelectron spectroscopy

A SSI SSX-100/206 spectrometer of Fisons was used for the XPS experiments. This spectrometer consists of a monochromatized microfocus Al X-ray source, an electron collection lens, a hemispherical analyser and a microchannel plate as detector. Details concerning this kind of spectrometer have been given previously [13]. The sample powders were pressed in stainless steel troughs (4 mm diameter) and placed on an aluminium carrousel. The samples were heated by a quartz lamp (max 120 °C) three times during 15 min under vacuum. The heating periods were separated by 30 min pauses for outgassing. The samples were then outgassed overnight under vacuum and introduced in the analysis chamber. The residual pressure during the analysis remained between (1 and 5) $\times 10^{-9}$ Torr. The Al monochromatized X-ray source was operated at 10 kV. A low energy flood gun (6 eV) with a Ni grid placed 3 mm above the samples was used to compensate for charging during measurements. For each sample, a survey spectrum was recorded, followed by detailed scans of C_{1s}, O_{1s}, N_{1s} + Ga_{Auger}, P_{2p}, Al_{2p}, Ga_{3p} and finally, C_{1s} again. The spectra were decomposed with the least-squares fitting routine with a Gaussian/Lorentzian ratio of 85/15 and after subtraction of a non-linear baseline. For the determination of the nitrogen atomic fraction, the contribution of the Ga_{Auger} peak ($L_2M_{45}M_{45}$) to the N_{1s} signal was subtracted. The atomic ratios were calculated from relative intensities corrected by the elemental sensitivity factors provided by the manufacturer. In the calculation of those factors, the Scofield's photoionization cross-section were used.

2.3. DRIFTS measurements

In situ DRIFTS spectra were collected in an infrared EQUINOX 55 spectrometer from Bruker with KBr optics and a MCT (Mecury Cadmium Telluride) cooled detector. Pure samples were placed inside a commercial controlled environmental chamber equipped with SeZn windows, attached to a diffuse reflectance accessory. The samples were heated from room temperature (RT) to 275 °C under a 30 ml/min inert gas flow (He, 99.999%). The temperature was increased manually at approximately 5 °C/min. Spectra were recorded (200 scans, 4 cm^{-1} resolution) after 30 min of stabilisation. The spectrum of an aluminum mirror was used as background.

2.4. FT-IR study of alcohol adsorption

Methanol and butan-1-ol spectra were recorded using a Nicolet Magna 550 spectrometer, with a DTGS (deuterated triglycine sulphate) detector. The powders were pressed into self-supporting disks (∼15 mg, disc surface 2 cm^2), placed in an IR cell connected to a vacuum line. The wafers were degassed at 300 °C for 30 min before analysis. After cooling to room temperature, a spectrum of the powder was recorded. The alcohols were then adsorbed at a pressure of 1 Torr at RT for 5 min. The cell was then evacuated at RT for 15 min (10^{-5} Torr). After the evacuation step, a spectrum was recorded (128 scans, 4 cm^{-1} resolution). The figures present spectra normalised to the same disk weight (10 mg for 2 cm^2).

2.5. Catalytic tests

The dehydration reactions were carried out at atmospheric pressure, in a quartz fixed bed micro-reactor (i.d. 10 mm), in up flow mode. The reactor was placed in a vertical furnace with temperature control. The real reaction temperature was measured by a thermocouple situated in the center of the reactor near the catalyst. Before reaction, the catalysts were sieved, and the particle size fraction of 100–200 μm was used. The catalyst mass was 100 mg, and the corresponding bed height was adjusted to 13 mm, by adding 200–500 μm glass balls.

Catalyst activation was performed in helium flow (30 ml/min) (Indugas 4.5), at reaction temperature for 2 h. The MgO and ZrO_2 catalysts were heated at higher temperature (550 °C) prior to the reaction, so as to remove H_2O and CO_2, known to be strongly adsorbed on base sites.

Helium, the carrier gas, was used to bring butanol into the vapour phase from a saturator held at 27 °C, for butan-2-ol (p.a., Jansen chimica), and 41 °C, for butan-1-ol (p.a. ACROS organics), which leads to a butanol partial pressure of 2.6 kPa in both cases. This helium/butanol gas reaction mixture passed through the reactor at a rate of 30 ml/min (WHSV = 1.3 h^{-1}). To prevent the condensation of butanol or reaction products, all lines from the saturator to the chromatograph were heated above 100 °C.

Unconverted butanol and the dehydration products were analysed by gas chromatography, using a Shimidazu Chrompac C-R3A chromatograph, equipped with a flame ionisation detector, with helium as carrier gas. A 50 m × 0.32 mm (RSL-160) capillary column was used for the separation of the various compounds. Water was not considered in the characterisation of the composition of the reaction mixture.

The specific activity, *r*, was defined as the number of butanol moles transformed in one second per square meter of specific surface area of the catalyst. The conversion (%), was defined as the ratio of the amount of converted butanol to the amount of butanol supplied at reactor inlet. The selectivity for each product (molar %) was defined as the molar ratio of each of them to all the detected products. We verified that the carbon balance was reached without significant error. For quantitative comparison between the catalysts, care was taken to ensure that the data were controlled neither by external nor internal diffusion.

3. Results

3.1. Catalytic tests

3.1.1. Butan-2-ol dehydration test reaction

The catalytic properties of the AlGaPON series of samples for butan-2-ol dehydration were investigated, at 200 °C and a weight hourly space velocity of 1.3 h^{-1} for 10 h. At initial time (15 min) (Table 3) the specific activity for butan-2-ol dehydration diminishes with nitrogen enrichment. With time

Table 3
Results of the butan-2-ol dehydration tests over AlGaPON (temperature: 200 °C; WHSV: 1.3 h^{-1}; initial conditions)

Catalyst	Specific activity (mol/m^2 s)	Yields (mol of product/m^2 s)			*Cis*/*trans* 2-butene ratio
		1-Butene	*Trans*-2-butene	*Cis*-2-butene	
AlGaPO	22.8×10^{-9}	3.9×10^{-9}	9.1×10^{-9}	9.6×10^{-9}	1.1
AlGaPON1	21.5×10^{-9}	4.3×10^{-9}	8.4×10^{-9}	8.8×10^{-9}	1.1
AlGaPON2	14.5×10^{-9}	3.0×10^{-9}	5.5×10^{-9}	6.1×10^{-9}	1.1
AlGaPON3	4.6×10^{-9}	0.9×10^{-9}	1.7×10^{-9}	2.0×10^{-9}	1.2
AlGaPON4	1.8×10^{-9}	0.4×10^{-9}	0.6×10^{-9}	0.8×10^{-9}	1.3

on stream, the activity of the nitrided samples progressively increases, the importance of the activation phenomenon being proportional to the nitrogen content of the samples (Fig. 1).

1-Butene, *trans*-2-butene and *cis*-2-butene are the only reaction products. The evolution of their distribution as a function of the nitrogen content of the catalysts is shown in Fig. 2: 1-butene selectivity slightly increases with nitridation, along with the *cis*/*trans*-2-butene ratio.

Comparison of the butene distribution obtained on the AlGaPO and on the most nitrided sample AlGaPON4 with those obtained on acid (SiO_2–Al_2O_3), amphoteric (Al_2O_3) and base (ZrO_2) catalysts under similar conditions is shown in Fig. 3. The histogram also shows the results obtained on the $AlPO_4$ phosphate precursor of the AlPON series of samples, whose reactivity was discussed in [8].

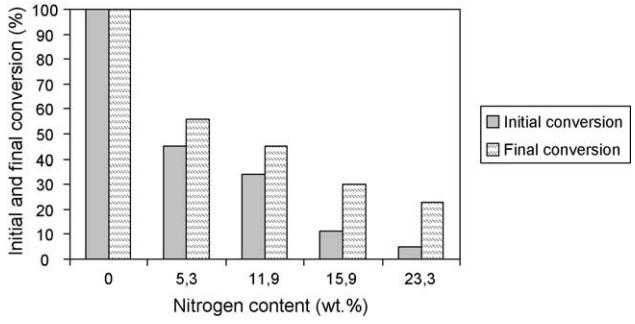

Fig. 1. Conversions measured after 15 min and after 10 h on stream as a function of the nitrogen content of AlGaPON for the dehydration of butan-2-ol (temperature: 200 °C; WHSV: 1.3 h^{-1}).

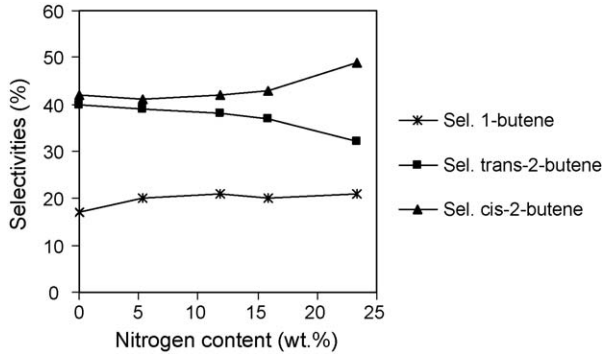

Fig. 2. Evolution of the selectivities as a function of the nitrogen content of AlGaPON for the dehydration of butan-2-ol (temperature: 200 °C; WHSV: 1.3 h^{-1}; initial conditions).

3.1.2. Butan-1-ol dehydration test reaction

Results for butan-1-ol dehydration tests on the AlGaPON series of samples are shown in Table 4. At initial time (15 min) the specific activity reaches a maximum for the AlGaPON1 sample, then progressively decreases with nitrogen enrichment. No significant activation phenomenon was observed with time on stream. At 275 °C, butenes (1-butene, *trans*-2-butene, *cis*-2-butene) and dibutylether were the only detected reaction products, their relative importance depending on the nitrogen content (Fig. 4). 1-Butene isomerises to 2-butene on the AlGaPO precursor, on the least and on the most nitrided samples, but not on the samples with intermediate nitrogen contents (Table 4).

Butene distributions on the AlGaPO precursor and on the most nitrided sample AlGaPON4 are compared to those obtained on acid (SiO_2–Al_2O_3) and base (MgO) references

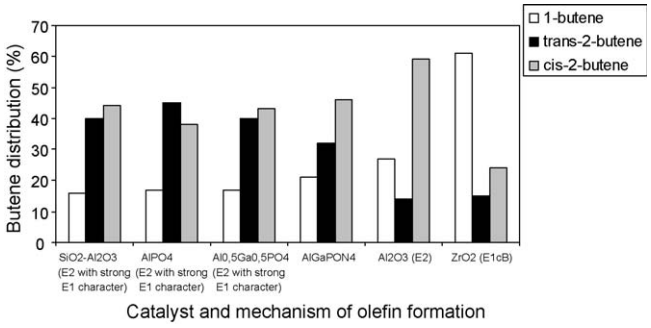

Fig. 3. Butene distribution obtained for butan-2-ol dehydration on the AlGaPO and AlGaPON4 and on reference oxides (temperature: 200 °C (300 °C for ZrO_2); WHSV: 1.3 h^{-1}; initial conditions). Reaction mechanisms, deduced from the butene distribution are shown in brackets.

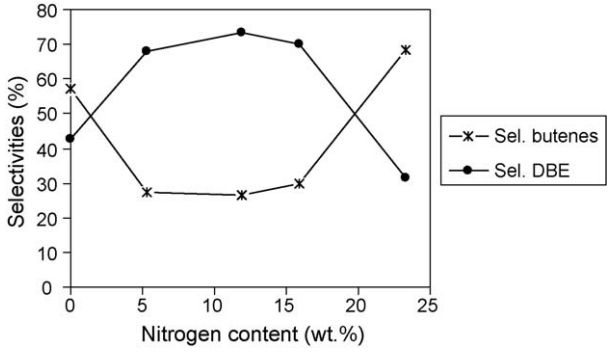

Fig. 4. Evolution of the selectivities for dibutylether (DBE) and for butenes (1-butene, *cis*-2-butene and *trans*-2-butene) as a function of the nitrogen content of AlGaPON for the dehydration of butan-1-ol (temperature: 275 °C; WHSV: 1.3 h^{-1}; initial conditions).

Table 4
Results of the butan-1-ol dehydration tests over AlGaPON (temperature: 275 °C; WHSV: 1.3 h^{-1}; initial conditions)

Catalyst	Specific activity (mol/m^2 s)	Yields (mol of product /m^2 s)				*Cis/trans* 2-butene ratio
		1-Butene	*Trans*-2-butene	*Cis*-2-butene	Dibutylether	
AlGaPO	18.0×10^{-9}	7.7×10^{-9}	1.3×10^{-9}	1.4×10^{-9}	3.8×10^{-9}	1.1
AlGaPON1	29.1×10^{-9}	7.9×10^{-9}	0.7×10^{-9}	0.8×10^{-9}	9.9×10^{-9}	1.1
AlGaPON2	20.0×10^{-9}	5.2×10^{-9}	0	0	7.4×10^{-9}	–
AlGaPON3	15.3×10^{-9}	4.6×10^{-9}	0	0	5.4×10^{-9}	–
AlGaPON4	7.6×10^{-9}	4.6×10^{-9}	0.2×10^{-9}	0.5×10^{-9}	1.2×10^{-9}	2.5

Table 5
Comparison of the product distribution on AlGaPO and AlGaPON2 at total conversion during butan-1-ol dehydration tests (temperature: 350 °C; WHSV: 1.3 h^{-1}; initial conditions)

Catalyst	AlGaPO	AlGaPON2
Conversion (%)	100	100
Selectivities (%)		
1-butene	60	66
Trans-2-butene	20	16
Cis-2-butene	20	16
Dibutylether	0	0
Butyraldehyde	0	2

Table 6
Nitrogen surface atomic percentages evaluated by XPS prior to and after butan-1-ol dehydration tests over AlGaPON4 sample

	Nitrogen surface atomic percentage	
	AlGaPON	AlPON
Fresh catalyst	30	23
Used catalyst	13	7
Relative nitrogen loss[a] (%)	57	70

Results obtained over AlPON sample tested in the same conditions are also shown for comparison (temperature: 275 °C; WHSV: 1.3 h^{-1};10 h tests).
[a] (N at.% prior test − N at.% after test)/N at.% prior test × 100.

under similar reaction conditions (Fig. 5). 1-Butene isomerises most strongly on acid (SiO_2–Al_2O_3) and strongly basic (MgO) catalysts. The *cis*/*trans* ratio is close to 1 for the acid-catalysed isomerisation and higher for the basic isomerisation.

The histogram also shows the results obtained on the $AlPO_4$ phosphate whose reactivity was discussed in [8].

The selectivities obtained at total conversion for an oxide and an oxynitride are shown in Table 5. The fraction of 1-butene isomerised to *cis*- and *trans*-2-butene is lower on the nitrided sample. In this sample, butyraldehyde is detected among the reaction products.

3.2. Post-test physico-chemical characterizations

3.2.1. XPS analysis

Nitrogen surface atomic percentages evaluated by XPS prior to and after butan-1-ol dehydration tests on the AlGaPON4 sample are shown in Table 6. In 10 h time, the relative nitrogen loss is 57%. Tested in the same conditions, a highly nitrided AlPON loses 70% of its superficial nitrogen species.

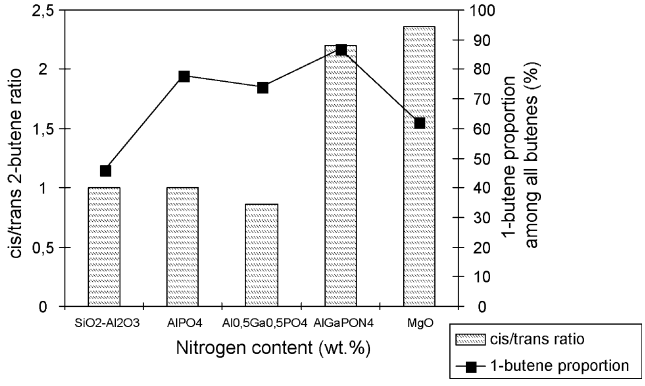

Fig. 5. Butene distribution obtained for butan-1-ol dehydration on the AlGaPO and AlGaPON4 and on reference oxides (temperature: 275 °C (400 °C for MgO); WHSV: 1.3 h^{-1}; initial conditions).

3.2.2. DRIFTS analysis

Fig. 6 presents the in situ DRIFTS spectra recorded on the AlGaPON4 sample prior to and after the dehydration tests. Assignment of the DRIFTS bands observed in the spectra are shown in Table 7. The spectrum of the used sample shows the

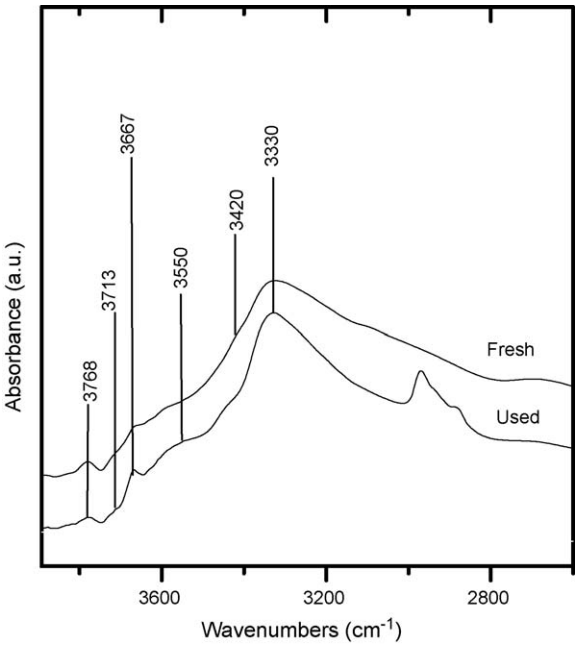

Fig. 6. In situ DRIFTS spectra of the AlGaPON4 sample recorded at 275 °C prior to and after the butan-1-ol dehydration test.

Table 7
Position (cm^{-1}) and assignments of the DRIFTS bands observed in the spectra of the AlGaPON4 oxynitride, according to Refs. [17,22]

Wavenumbers (cm^{-1})	Assignments
3767	ν(OH) in tetrahedral Al–OH
3713	ν(OH) in tetrahedral Ga–OH
3667	ν(OH) in tetrahedral P–OH
3550	ν(OH) in H-bonded–OH
3420	ν_s(NH) in M–NH_2
3330	ν(NH) in M–NH–M

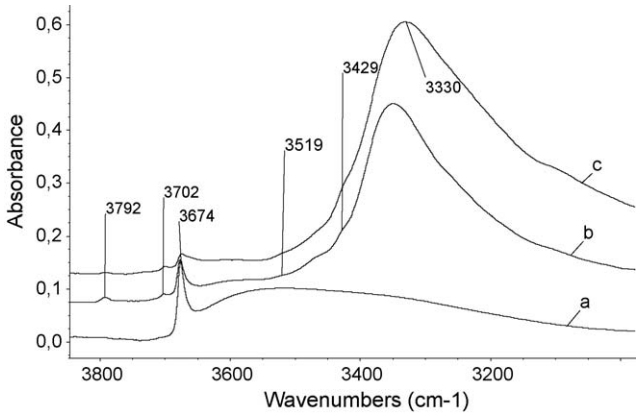

Fig. 7. FT-IR spectra of AlGaPON oxynitrides evacuated at 300 °C: AlGaPO (a), AlGaPON2 (b), AlGaPON4 (c).

presence of absorption bands in the 2800–3100 cm^{-1} energy range corresponding to ν(C–H) vibrations in adsorbed butanol.

3.3. FT-IR study of alcohol adsorption

To evidence the nature of the surface species present on AlGaPON and show the influence of nitridation on their relative concentrations, FT-IR spectra of the AlGaPO precursor and two nitrided samples (AlGaPON2 and AlGaPON4) were recorded after a thermal treatment of 300 °C. The spectra are present in Fig. 7. The evolution of the IR band area of the ν(OH) in P–OH groups (3674 cm^{-1}), ν(OH) in Ga–OH groups (3702 cm^{-1}),

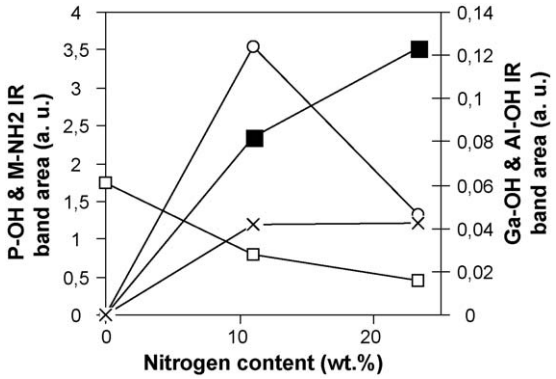

Fig. 8. Evolution of the IR band area of the ν(OH) in P–OH groups (□), ν(OH) in Ga–OH groups (×), ν(OH) in Al–OH groups (○), and δ(HNH) in M–NH_2 groups (■) as a function of the total nitrogen content of AlGaPON.

ν(OH) in Al–OH groups (3792 cm^{-1}), and δ(HNH) in M–NH_2 groups (1555 cm^{-1}) as a function of the total nitrogen content of AlGaPON is shown in Fig. 8.

Methanol was adsorbed on the surface of AlGaPO, AlGaPON2 and AlGaPON4 samples, at room temperature. The difference spectra, obtained by subtracting the reference spectra recorded after evacuation of the samples at 300 °C (as presented in Fig. 7) from the spectra recorded after methanol adsorption, are presented in Fig. 9.

Results of butan-1-ol adsorption at room temperature on the AlGaPON4 sample are presented in Fig. 10. This figure shows the spectra of the sample evacuated at 300 °C before and after butan-1-ol adsorption as well as the difference spectrum.

4. Discussion

4.1. Influence of nitridation on the elimination mechanism

4.1.1. For butan-2-ol dehydration

Dehydration of butan-2-ol to butenes can be executed with most solid acid catalysts as well as solid base catalysts. Butene distribution is one of the most significant clues to distinguish the elimination mechanism taking place on the surface. Dehydration over acid catalysts (E1 mechanism) generally yields Saytzeff products (i.e. formation of 2-olefins), while

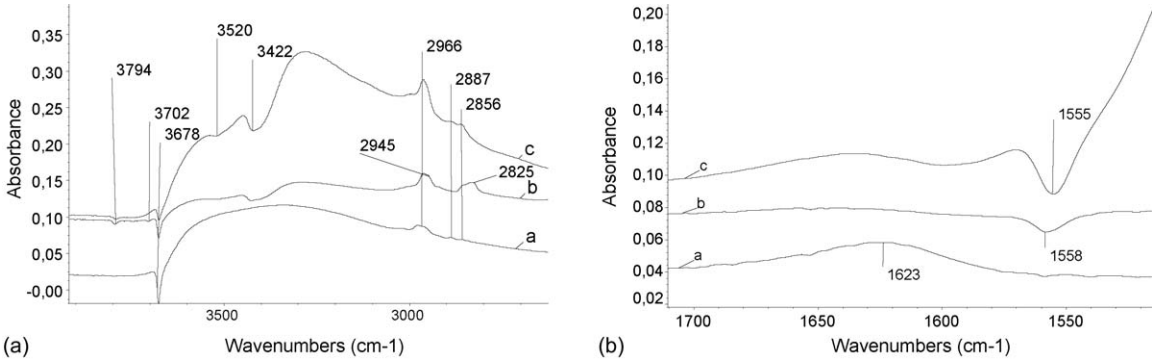

Fig. 9. Difference FT-IR spectra obtained after methanol adsorption and evacuation at RT for 15 min on the AlGaPO (a), AlGaPON2 (b) and AlGaPON4 (c) oxynitrides evacuated at 300 °C. Spectra are displayed in two regions: (A) 3900–2600 cm^{-1}; (B) 1700–1500 cm^{-1}.

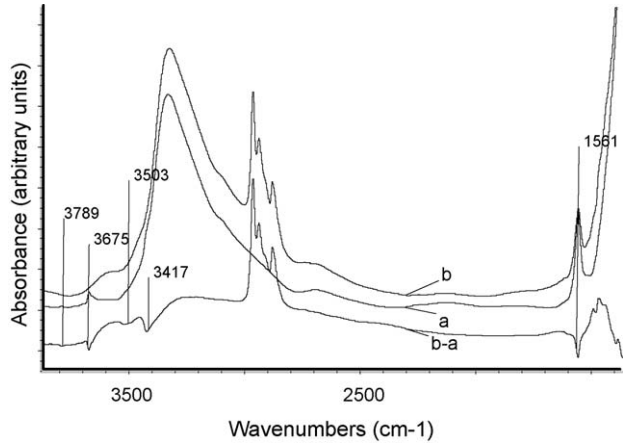

Fig. 10. FT-IR spectra of the oxynitride AlGaPON4 evacuated at 300 °C before (a), after (b) butan-1-ol adsorption and evacuation at RT and difference spectrum (b − a).

dehydration over basic oxides (E1cB mechanism) yields Hofmann elimination products (i.e. formation of 1-olefins). An intermediate situation will be found for the concerted elimination (E2 mechanism), which consists in a one-step concerted reaction that proceeds at the intervention of both acid and base surface sites.

A further indication of the presence of base sites on the surface is the occurrence of dehydrogenation of butan-2-ol to 2-butanone, which occurs on strong base sites. It was only observed on ZrO_2 and MgO, our most basic references, and not on AlGaPON.

In order to determine which mechanism dominated butan-2-ol elimination on the precursor AlGaPO, we compared the butene distribution obtained on this sample and on a typical E1 oxide (silica–alumina), E2 oxide (alumina) and E1cB oxide (ZrO_2) (Fig. 3). Butene distribution on the AlGaPO precursor is very close to that obtained on silica–alumina, and hence the mechanism of butan-2-ol elimination on this sample certainly presents a strong E1 character. The same conclusion is reached for the $AlPO_4$, precursor of the AlPON series of samples [8]. Upon nitridation (Fig. 2), the selectivity for 1-butene slightly increases. This indicates that some base sites, strong enough to activate the C–H bond at C1 position are created upon nitridation. Their number is weak, however, as even for the most nitrided sample AlGaPON4, the selectivity for 1-butene is lower than that obtained on alumina (Fig. 3). Hence, on AlGaPON, activities and selectivities are mainly governed by the strength and the density of the acid sites.

4.1.2. For butan-1-ol dehydration

4.1.2.1. The intramolecular dehydration of butan-1-ol to 1-butene. The intramolecular dehydration of butan-1-ol to 1-butene can occur through a carbonium ion (E1), a carbanion (E1cB) or through a concerted mechanism (E2), as discussed above. 1-Butene can subsequently isomerise to *cis*/*trans*-2-butene on acid or base sites, a high *cis*/*trans* ratio being observed for the base-catalysed isomerisation, a ratio close to 1 being observed for the acid-catalysed isomerisation.

- On the acid SiO_2–Al_2O_3 reference, the carbonium ion mechanism E1 can explain product distribution: 57% of 1-butene is isomerised to *cis*/*trans*-2-butene, the *cis*/*trans* ratio being equal to 1 (Fig. 5).
- On the base MgO reference, the carbanion E1cB mechanism can explain product distribution: 38% of 1-butene is isomerised to *cis*/*trans*-2-butene, the *cis*/*trans* ratio being higher than 2.
- On the AlGaPO precursor, only 26% of 1-butene is isomerised, which suggests for butan-1-ol, a concerted mechanism E2, rather than the carbonium ion mechanism E1 observed for butan-2-ol.

Because butan-1-ol is less basic than butan-2-ol, it is proposed that the acid sites present on the AlGaPO precursor are not strong enough to catalyse its dehydration through the carbonium ion mechanism E1. Butan-1-ol is also less reactive than butan-2-ol, which explains that higher reaction temperatures are necessary to reach similar conversions. The same conclusions were reached for the $AlPO_4$, precursor of the AlPON series of samples [8].

With nitridation, the fraction of 1-butene isomerised to 2-butene is still reduced and the *cis*/*trans* ratio increases up to 2, indicating an increase of the base character of the samples with nitrogen enrichment (Table 4, Fig. 5).

4.1.2.2. The intermolecular dehydration of butan-1-ol to DBE. The intermolecular dehydration of butan-1-ol to dibutylether (DBE) necessitates the simultaneous activation of two alcohol molecules on adjacent acid–base sites, as evidenced in Ref. [14]. On SiO_2–Al_2O_3 and MgO references, no DBE is formed, which confirms the carbonium ion (E1) and carbanion (E1cB) mechanisms proposed for the intramolecular dehydration of butan-1-ol to 1-butene.

On AlGaPO and AlGaPON, on the opposite, DBE is a major reaction product which confirms the existence of both acid and base active sites on the catalyst surface, able to activate simultaneously acid and base functional groups in the reacting molecules.

The selectivity for DBE (Fig. 4), as well as the DBE yields (Table 4) are increased at the beginning of nitridation, pass by a maximum for intermediate nitrogen contents and decrease for the most nitrided samples. A similar trend was observed for the series of AlPON samples [8].

4.1.2.3. The dehydrogenation of butan-1-ol to butyraldehyde. From a strictly acid–base point of view, the dehydrogenation reaction of alcohols occurs on strongly basic catalysts, such as MgO or CaO. However, on certain families of catalysts a redox mechanism can also be envisaged. The weak butyraldehyde formation observed on the AlGaPON2 sample (Table 5) could be ascribed either to the formation of a weak number of strong basic sites on the surface with nitridation, or to the increase of the gallium dehydrogenation properties with nitridation [9]. On AlPON, butyraldehyde was never observed, whatever the reaction temperature [8].

4.2. Stability of the surface nitrogenous species during the reaction

During the butan-2-ol dehydration tests over AlGaPON, the conversion increases with time on stream, the relative increase being proportional to the nitrogen content of the samples (Fig. 1).

From Fig. 6, it appears that this activity increase could be linked to the creation of new acid P–OH groups (ν(OH) groups in tetrahedral P–OH at 3667 cm^{-1}). Their formation during the catalytic test most certainly results from the hydrolysis of P–N bonds (in P–NH_2, P–NH–M or P–N < species). The Brønsted acid character of P–OH groups in AlGaPON has been previously evidenced through a FT-IR study of pyridine adsorption [4]. The hydrolysis mechanism of P–N bonds in AlPON, induced by the presence of small concentrations of gaseous water, has been thoroughly studied in [15].

The creation of new P–OH species during the tests over AlGaPON does not significantly influence their activity for the conversion of butan-1-ol, which is another indication that the superficial species involved in butan-1-ol and butan-2-ol dehydration are not the same.

We know, from previous studies [11], that the substitution of aluminium by gallium atoms in AlGaPON has a very significant impact on the nitridation process:

- The minimum nitridation temperature decreases when the gallium content of the sample increases. For instance, the minimum nitridation temperature of an $AlPO_4$ oxide is approximately 600 °C, while the minimum nitridation temperature of a $GaPO_4$ oxide is approximately 400 °C.
- The amount of nitrogen incorporated in the phosphate structure under fixed reaction conditions increases with gallium enrichment of the samples.

From the comparison of the relative superficial nitrogen loss after 10 h on stream on AlPON and AlGaPON (Table 6), it is also apparent that gallium help stabilize the nitrogeneous superficial species during a catalytic test performed in the presence of gaseous water.

4.3. Correlation of the specific activities to the acid–base properties of AlGaPON

From the analysis of the product distribution, we concluded that the E1 mechanism controls product distribution during butan-2-ol dehydration over AlGaPON. To explain the decrease of the specific activity (r) with nitridation we invoked a decrease of the number of acid sites with nitrogen enrichment. This hypothesis is confirmed by the good similarity between the specific activity decrease and the decrease in the number of acid sites probed at 35 °C by ammonia [4] as a function of the nitrogen content of the samples (Fig. 11).

The decrease in the number of acid sites is due to the simultaneous decrease of the number of Brønsted and Lewis acid sites:

(i) The replacement of the acid P–OH groups by P–NH_x species during nitridation explains the decrease in the number of Brønsted acid sites. This replacement is evidenced in Figs. 7 and 8. There is no correlation between the total number of acid sites evaluated by ammonia chemisorption (Fig. 11) and the superficial concentration of Al–OH and Ga–OH groups (Figs. 7 and 8).

(ii) The decrease in the number of Lewis acid sites induced by nitridation is due to the neutralisation of the coordinatively unsaturated ions by NH_x species and/or the substitution of oxygen atoms by nitrogen around coordinatively unsaturated cations, which reduces their positive charge, and hence, their tendency to attract electrons.

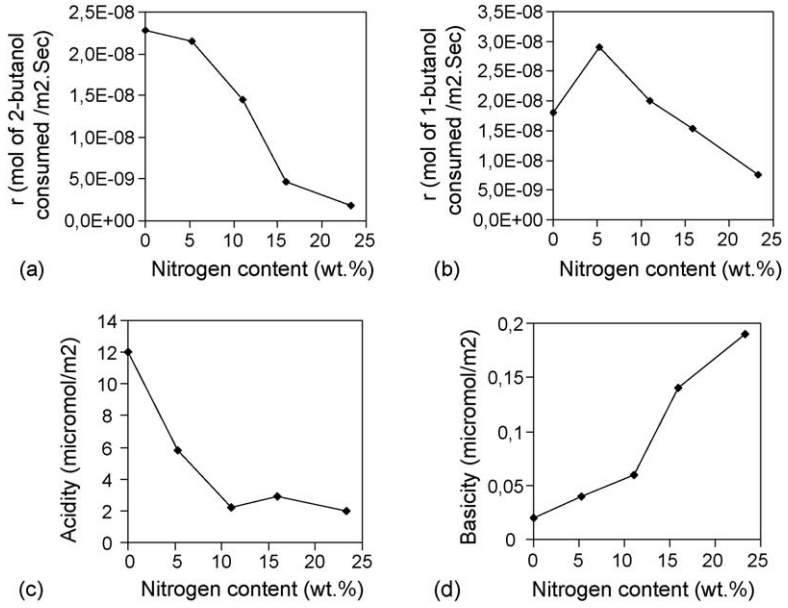

Fig. 11. Evolution of the specific activities r as a function of the nitrogen content of AlGaPON for butan-2-ol (a) and butan-1-ol (b) dehydration tests; correspondence between the catalytic activities and the acid [4] (c)/base [5] (d) properties of the catalysts.

As concerns butan-1-ol dehydration, we concluded from the analysis of product distribution that the reaction rate was governed by the density of coupled acid–base sites. The evolution of the reaction rate *r* with nitrogen enrichment for this reaction is neither correlated to the acidity measurements performed by ammonia chemisorption, nor to the basicity measurements performed by sulphur dioxide microcalorimetry [5]. The reaction rate reaches a maximum for an intermediate nitrogen content which leads us to propose that the weakly nitrided samples posses an optimum density of coupled acid and base sites for butan-1-ol dehydration.

To determine the nature of the coupled acid and base sites interacting with butan-1-ol, we recorded the FT-IR spectra of AlGaPO and AlGaPON prior to and after methanol (Fig. 9) and butan-1-ol (Fig. 10) adsorption.

On the oxide, methanol adsorption results from interaction with surface P–OH hydroxyl groups, as can be deduced from the important changes in the νOH band at 3678 cm^{-1}. In the 3100–2800 cm^{-1} region, methanol adsorption gives rise to several C–H stretching bands. The CH_3 deformation region, as well as the C–O stretching region cannot be exploited due to the strong intensity of the phosphate structural bands below 1500 cm^{-1}.

Interaction between methanol and P–OH groups can result from hydrogen-bonding or from an exchange reaction (Eq. (3)):

$$P{-}OH + CH_3OH \rightarrow P{-}OCH_3 + H_2O \quad (3)$$

Water production upon methanol adsorption over the AlGaPO precursor is evidenced by the positive band appearing in the spectrum around 1623 cm^{-1} (δ(HOH) in adsorbed water) (Fig. 9).

With nitridation, the number of methanol molecules adsorbed on the surface increases, as evidenced by the development of the C–H stretching bands in the 3100–2800 cm^{-1} region. The relative intensities of the bands in this region are strongly affected by nitridation. In particular, a band component appears at 2825 cm^{-1} in the spectrum of methanol adsorbed over AlGaPON2. According to Lavalley [16], a shift of the ν(CH) wavenumbers to lower values upon primary alcohol adsorption might be an indication of dissociative adsorption. The proper assignment of the C–H stretching modes is not trivial, however, and it is difficult to elaborate further on this result.

The increase in the number of adsorbed methanol molecules with nitridation is most certainly due to the creation of new base sites. From previous SO_2 and $CDCl_3$ FT-IR adsorption studies [17], we know that the $-NH_2$ groups are able to interact with acidic probes. Indeed, all the IR bands characteristic of $-NH_2$ groups are perturbed by methanol adsorption (ν(NH) bands at 3520 (ν_{as}) and 3422 (ν_s) as well as δ(HNH) band at 1558 cm^{-1}). As already observed with SO_2 and $CDCl_3$ methanol adsorption does not modify the –NH– band in an important way.

The Ga–OH and Al–OH groups, whose density is maximum over the AlGaPON2 sample, are also in interaction with the adsorbed methanol molecules, as evidenced by the perturbation of the ν(OH) in Ga–OH groups (3702 cm^{-1}) and ν(OH) in Al–OH groups (3794 cm^{-1}) bands.

The adsorption of butan-1-ol on the AlGaPON4 sample results from similar interactions.

The optimum activity of the weakly nitrided samples for butan-1-ol dehydration could thus result from an optimum density of M–OH (M = P, Ga, Al) and $M–NH_2$ groups at low nitrogen contents. However, this explanation does not take into account the possible interactions of butan-1-ol with Lewis acid sites, basic framework oxygen or nitride ions, which could not be revealed by our FT-IR study.

5. Conclusion

The presence of coupled acid-base sites over AlGaPON was postulated in the past to explain their good performances as support for platinum for the dehydrogenation of isobutane to isobutene. Besides, it could also explain the absence of correlation between the catalytic activity of those samples for the Knoevenagel condensation between benzaldehyde and malononitrile and the number of base sites determined by SO_2 microcalorimetry experiments.

In order to show the existence of acid–base pairs able to interact simultaneously with reactant molecules on the surface of AlGaPON, and to study the evolution of the number of these sites with the nitrogen enrichment, we studied in parallel the activity and stability of those catalysts for the dehydration of linear alcohols (butan-1-ol and butan-2-ol), because the inter- and intra-molecular dehydration of those alcohols can occur through concerted acid–base mechanisms.

Product distribution evidences that butan-2-ol is dehydrated through an E1 mechanism over AlGaPON. Reaction rates are correlated with the ammonia chemisorption experiments for the tested catalysts.

Butan-1-ol dehydration experiments show that AlGaPON possess conjugated acid–base sites able to activate simultaneously two alcohol molecules, and to catalyse the intermolecular dehydration of butan-1-ol to dibutylether. The density of bifunctional acid–base sites able to catalyse butanol dehydration through a concerted mechanism is increased by nitridation, but an optimum is found for intermediate nitrogen contents.

Differences in butan-1-ol and butan-2-ol dehydration mechanisms are due to differences in the acidity–basicity of those two alcohols. The basicity of butan-2-ol being higher than that of butan-1-ol, its dehydration through an acid mechanism is favoured.

FT-IR of adsorbed alcohols allowed us to identify $M–NH_2$ species as one type of base site activating alcohol molecules over AlGaPON oxynitrides.

Acknowledgements

The authors thank Pierre Eloy and Mehdi Hamrouni (Unité de Catalyse et Chimie des Matériaux Divisés, Université Catholique de Louvain, Belgium) for the help provided in the recording and processing of XPS spectra as well as the help provided in performing the catalytic tests. They are grateful to Valérie Ruaux (Laboratoire de Catalyse et Spectrochimie de

Caen, France) for the help provided in the recording and interpretation of the IR spectra.

They would also like to thank the Fonds National de la Recherche Scientifique (FNRS) for the fellowship awarded to Stéphanie Delsarte.

References

[1] P. Grange, Ph. Bastians, R. Conanec, R. Marchand, Y. Laurent, L. Gandia, M. Montes, J. Fernandes, J.A. Odriozola, in: G. Poncelet, et al. (Eds.), Preparation of Catalysts VI, Scientific Bases for the Preparation of Heterogeneous Catalysis, Elsevier, Amsterdam, 1995, p. 381.
[2] P. Grange, Ph. Bastians, R. Conanec, R. Marchand, Y. Laurent, Appl. Catal. A 114 (1994) L191.
[3] A. Massinon, J.A. Odriozola, Ph. Bastians, R. Conanec, R. Marchand, Y. Laurent, P. Grange, Appl. Catal. A 137 (1996) 9.
[4] S. Delsarte, V. Peltier, Y. Laurent, P. Grange, Stud. Surf. Sci. 118 (1998) 869.
[5] S. Delsarte, A. Auroux, P. Grange, Phys. Chem. Chem. Phys. 2 (12) (2000) 282.
[6] N. Fripiat, P. Grange, J. Chem. Soc., Chem. Commun. (1996) 1409.
[7] N. Fripiat, R. Conanec, A. Auroux, Y. Laurent, P. Grange, J. Catal. 167 (1997) 543.
[8] S. Delsarte, P. Grange, Appl. Catal. A: Gen. 259 (2004) 269.
[9] S. Delsarte, F. Maugé, P. Grange, J. Catal. 202 (2001) 1.
[10] K. Kearby, in: Proceedings of the Second International Congress Catalysis, Technip, Paris, (1961), p. 2567.
[11] V. Peltier, R. Conanec, R. Marchand, Y. Laurent, S. Delsarte, E. Guéguen, P. Grange, Mater. Sci. Eng. B 47 (1997) 177.
[12] F.F. Grekov, J. Guyader, R. Marchand, J. Lang, Rev. Chim. Miner. 15 (1978) 341.
[13] R.L. Chaney, Surf. Interface Anal. 10 (1987) 36.
[14] P. Berteau, M. Ruwet, B. Delmon, Bull. Soc. Chim. Belg. 94 (11–12) (1985) 859.
[15] M.A. Centeno, M. Dubois, P. Grange, J. Phys. Chem. 102 (35) (1998) 6835.
[16] J.C. Lavalley, Catal. Today 27 (1996) 377.
[17] S. Delsarte, F. Maugé, J.C. Lavalley, P. Grange, Catal. Lett. 68 (2000) 79.
[18] A. Massinon, E. Guéguen, R. Conanec, R. Marchand, Y. Laurent, P. Grange, Stud. Surf. Sci. Catal. 101 (1996) 77.
[19] T. Ogihara, H. Nakajima, T. Yanagawa, N. Ogata, K. Yoshida, J. Am. Ceram. Soc. 74 (9) (1991) 2263.
[20] Y.T. Moon, D.K. Kim, C.H. Kim, J. Am. Ceram. Soc. 78 (4) (1995) 103.
[21] Ph. Courty, H. Ajot, Ch. Marcilly, B. Delmon, Powder Technol. 7 (1973) 21.
[22] S. Delsarte, M.A. Centeno, P. Grange, J. Non-Cryst. Solids 297 (2002) 189.